Computers and Concrete, *Vol. 14, No. 6 (2014) 767-783*
DOI: http://dx.doi.org/10.12989/cac.2014.14.6.767

Impact of composite materials on performance of reinforced concrete panels

Sherif A. Mazek*[1] and Ashraf A. Mostafa[2a]

[1] *Civil Engineering Department, Military Technical College, Cairo, Egypt*
[2] *Egyptian Engineering Department, Cairo, Egypt*

(*Received April 30, 2014, Revised October 6, 2014, Accepted November 11, 2014*)

Abstract. The use of composite materials to strengthen reinforced concrete (RC) structures against blast terror has great interests from engineering experts in structural retrofitting. The composite materials used in this study are rigid polyurethane foam (RPF) and aluminum foam (ALF). The aim of this study is to use the RPF and the ALF to strengthen the RC panels under blast load. The RC panel is considered to study the RPF and the ALF as structural retrofitting. Field blast test is conducted. The finite element analysis (FEA) is also used to model the RC panel under shock wave. The RC panel performance is studied based on detonating different TNT explosive charges. There is a good agreement between the results obtained by both the field blast test and the proposed numerical model. The composite materials improve the RC panel performance under the blast wave propagation.

Keywords: displacements; field blast test; finite element analysis; blast wave; composite materials; RC panels; TNT explosive charge

1. Introduction

Technologies provide blast protection for civilian structures (Aimone 1982; Liu and Katsabanis 1997; Fayad 2009; Mohamad 2006; Schueller 1991; Zhang and Valliappan 1990). There is a need to understand both dynamic interaction of blast loading with structures and shock mitigating mechanisms. Traditional lightweight materials such as the rigid polyurethane foam (RPF) and the aluminum foam (ALF) are effective materials for blast protection applications because of their ability to mitigate shock blast wave transferred to structures due to terrorism (Liu and Katsabanis 1997; Gustafsson 1973; Technical Manual TM 5-885-1 1986; Technical Manual TM 5-1300 2008).

To better understand structural damage under dynamic conditions, there are many researches to study civilian structures (Fayad 2009; Mohamad 2006; Beshara 1994; Liane and Hedman 1999; Smith and Hetherington 1994). The composite structures become an engineering challenge to understand their performance against blast effect.

It is very expensive to conduct field blast tests in every site and sometimes it is impossible to

*Corresponding author, Associate Professor, E-mail: samazek@yahoo.com
[a] Ph.D., E-mail: agwa100@gmail.com

http://www.techno-press.org/?journal=cac&subpage=8 ISSN: 1598-8198 (Print), 1598-818X (Online)

carry out such field tests due to safety and environmental constraints (Dharmasena *et al*. 2008; Hao *et al*. 1998). However, a reliable numerical model validated against measured field data is an effective tool to analyze the structure performance under blast effect (Dharmasena *et al*. 2008; Hao *et al*. 1998; Ming 2008).

Chen and Chen (1996) investigated the dynamic soil-structure interaction phenomenon involved in shallow-buried flexible plate under impact load. They used the experimental and the numerical works to study the performance of the buried structure. Lu *et al*. (2005) used a fully coupled numerical model to simulate the response of buried concrete structure under subsurface blast. The responses of the buried structure obtained by 2-D numerical model at different points were compared by those obtained by 3-D numerical model. Trelat *et al*. (2007) studied impact of shock wave on structure due to explosion at altitude. They improved the understanding of interaction of blast waves with both ground and structure using both the FEA and the experimental work. Luccioni *et al*. (2009) studied craters produced by underground explosions. They discussed the accuracy of numerical simulation of craters produced by underground explosions. Ha *et al*. (2011) used carbon fiber reinforced polymer (CFRP) to strengthen structures against blast load. They conducted an experimental work on CFRP to strengthen RC panels under blast loading. Mazek and Mostafa (2013) used the rigid polyurethane foam (RPF) to strengthen sandwich steel structure under blast load. The field blast test was conducted. They used the finite element analysis (FEA) to model the sandwich steel structure strengthened by the rigid polyurethane foam under shock wave. Mazek (2014) used the pyramid cover system (PCS) to strengthen sandwich steel structure under blast load. The field blast test was conducted. The finite element analysis (FEA) was used to model the sandwich steel structure strengthened by the PCS under shock wave.

In the present study, the performance of the reinforced concrete (RC) panels strengthened by composite materials is highlighted under the impact of the blast wave effect. The 3-D numerical model is proposed using finite element analysis (FEA) to study the composite materials to strengthen the RC panels, as shown in Fig. 1. The RPF and the ALF are used to study blast mitigation based on constant sheet thicknesses of the RPF and the ALF. Field blast test is also conducted to record pressure-time history of blast effect hitting the RC panel and to record maximum displacement at the centre point of the RC panel.

The study presents a comparison between the results obtained by both the field blast test and the numerical model to validate the accuracy of the 3-D finite element analysis (FEA). The FEA is used to study the performance of the RC panel strengthened by the RPF and the ALF. The constitutive model for this analysis contains elasto-plastic materials. An elasto-plastic model is also employed to represent the RPF layer and the ALF layer. A nonlinear-inelastic model is also employed to represent the RC panel. Current codes and regulations to estimate blast wave intensities due to outdoor blasting are also used in this study based on empirical methods (Gustafsson 1973; Technical Manual TM 5-1300 2008; Remennikov 2003). These empirical methods were obtained from observations and measurements in field blast tests.

The finite element model takes into account the effects of the blast load, the RC panel, the RPF, and the ALF. The effects are expressed in terms of the maximum displacement at the centre of the RC panel as the explosive wave propagates. The 3-D nonlinear FEA is conducted to study the impact of the composite materials on the RC panel performance based on different TNT explosive charges. The behavior of the RC panel is investigated under the blast waves obtained from detonating 1-kg, 2-kg, and 3-kg TNT explosive charges at a stand-off distance (R) of 1 m.

Numerical results obtained by the FEA are compared with the data obtained from the field blast test. The numerical model can well predict the blasting-induced pressure on the RC panel. Maximum displacements of the RC panels are recorded and computed by the authors.

2. Field blast test

In the present study, the field blast test is conducted to study the RC panel performance based on different TNT explosive charges. The control RC panels are prepared and tested in this study. The thickness of the control RC panel is 10 cm, as shown in Fig. 1. The control RC panel strengthened by the RPF are also prepared and tested, as shown in Fig. 2. The control RC panel strengthened by the ALF are also prepared and tested, as shown in Fig. 2. The thickness of the RPF is considered to be 10 cm and the thickness of the ALF is 5 cm, as shown in Fig. 2.

The RC panel is subjected to 1-kg, 2-kg, and 3-kg TNT explosive charges. The RC panels strengthened by both the RPF layer and the ALF layer are also tested under different TNT explosive charges.

The previous specimens are prepared and assembled with special requirements to be tested against TNT explosives. A test rig is prepared and used to simulate the RC panel boundary in free air. However, the test rig also needs some precautions to satisfy boundary conditions for free air explosion. The dimensions of the test rig are 1.03 m × 1.03 m × 1 m, as shown in Fig. 3. The members of the test rig are steel angles. These angle members are welded face to face. Angles (70 mm × 7 mm) are welded in vertical and horizontal directions so as to support the tested specimens, as shown in Fig. 3. The height of the supporting angles is 1.0 m, as shown in Fig. 3. The corners of the steel frame for the test rig are braced by steel angles (70 mm x 7 mm), as shown in Fig. 3.

The sensor interface PCD-30A is a voltage meter that is connected with the personal computer so as to record pressure-time history hitting the RC panel due to blast effect, as shown in Fig. 4. The maximum displacements of the specimens are also measured under blast loading. LVDTs are placed at the centre of the RC panel. The sensors are used to record maximum displacement at the centre of the RC panel. This device is capable of measuring voltage which is recorded and attached to control software. This system can measure four channels. The sensors are also attached on the center of the specimen’s bottom surface (RC panel). Fig. 4 shows the field instrumentation devices.

The RC panel is subjected to blast pressure recorded at the case of 2-kg TNT explosive charge, as shown in Fig. 5. The high speed camera is also used to capture photos at 15000- 20000 frames/s. The photos of explosion with TNT charge of 2 kg are shown in Fig. 6.

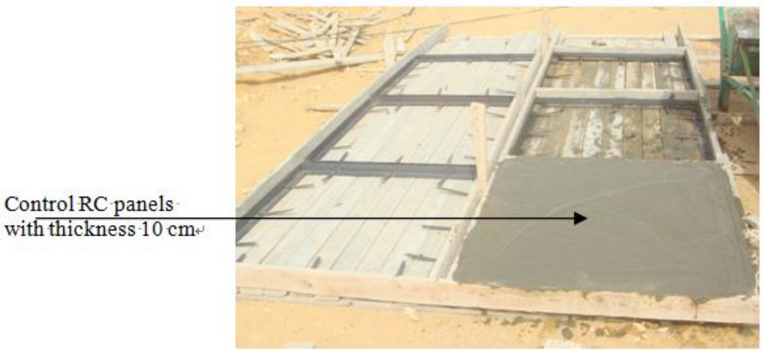

Fig. 1 Assembled reinforced concrete (RC) panels (Control RC panel)

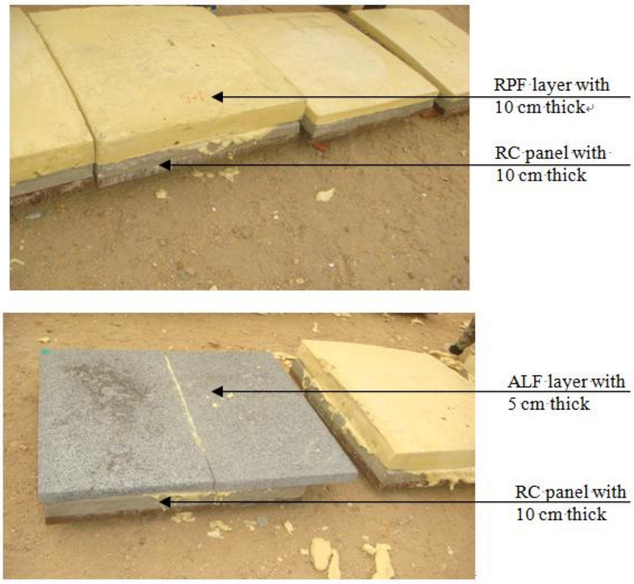

Fig. 2 Assembled reinforced concrete (RC) panels strengthened by the RPF and the ALF

Fig. 3 Test rig

Field instrumentation devices
Measurement sensors

Fig. 4 Field blast system measurement devices

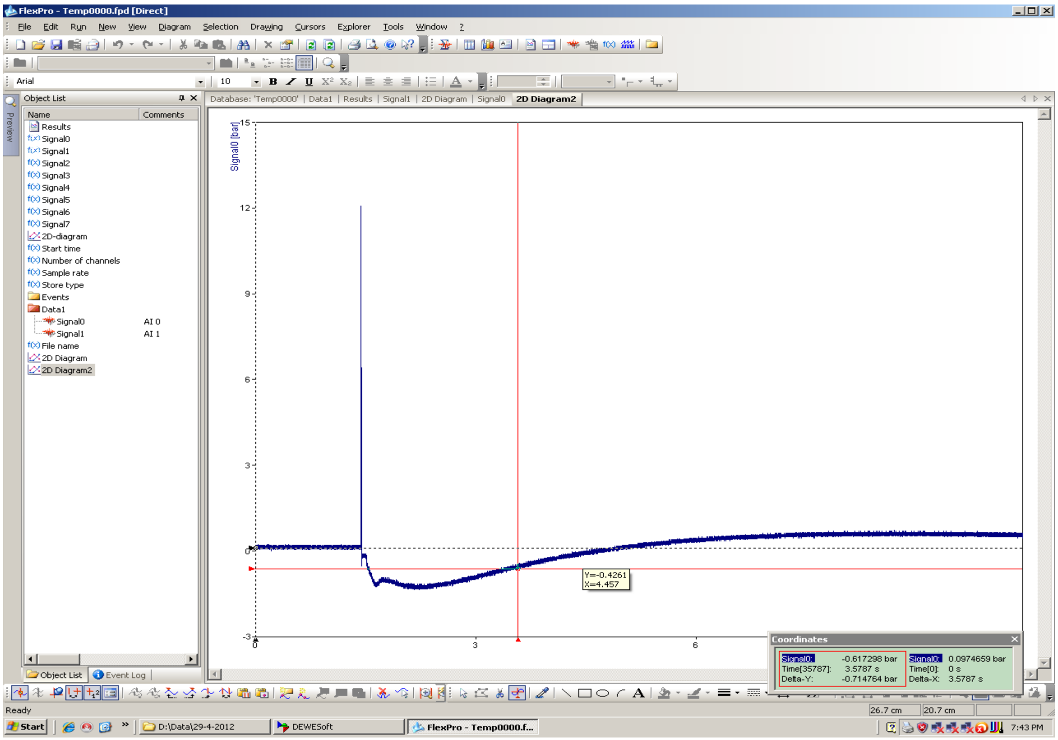

Fig. 5: Recorded pressure-time history hitting the RC panels using 2 kg-TNT explosive

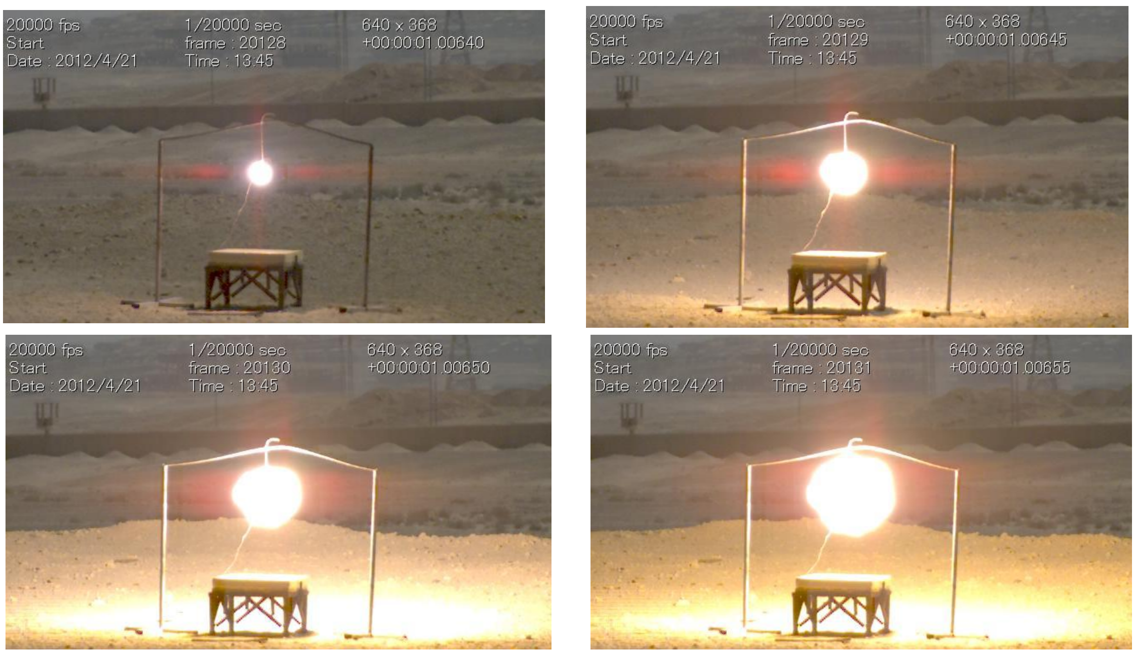

Fig. 6 Explosive scene by 3-kg TNT explosive

Fig. 6 Continued

3. Numerical model

The finite element computer program (COSMOS/M) is used in the present study. The finite element model (FEM) takes into account the effects of the non-linear properties of the composite materials (the RPF and the ALF), the blast effect generated by TNT explosive, and the non-linear properties of the RC panel. The RC panel, the composite layer, and the interface medium are simulated using appropriate finite elements. Figs. 1 and 2 show the typical section of the prepared RC panel subjected to blast effect. The numerical modeling of the prepared concrete system must reflect the characteristic of the composite layer and the RC panel. In addition, the interface between the composite material and the RC structure should be idealized in the numerical model.

The RC panel, the RPF layer, and the ALF layer are modeled by the modified isotropic damage model and simulated by Lagrange processor (Hao *et al*. 1998; Wu *et al*. 1999), as shown in Fig. 7. It should be noted that viscous damping effect is neglected in the numerical simulation as its influence on high velocity explosion-type responses is insignificant (Hao *et al*. 1998; Wu *et al*. 1999).

3-D solid elements are used for modeling the composite layer and the RC panel, as shown in Fig. 7. Eight-node solid elements are adopted to simulate behavior of the composite layer and the RC panel. The 3-D cubic solid element interface is used between the composite material layer and the RC panel to ensure the compatibility conditions at the interface between them as well as the associated stress and strains along the interface surface. The edge at the bottom plane of the mesh is represented by a steel angle and the movement at this plane is restrained in all directions. The 3-D finite element mesh is shown in Fig. 7.

The mechanical properties of concrete are Poisson's ratio $\nu = 0.18$; averaged mass density of concrete = 2520 kg/m^3; elastic modulus E= 220 t/cm^2; compressive strength f_n= 500 kg/cm^2; and strain to failure of concrete ε_f = 0.001. The shear modulus of the concrete mass depends on the elastic modulus E and Poisson's ratio ν .

The mechanical properties of the RPF and the ALF is tested and obtained by the authors. The mechanical properties of the RPF layer are Poisson's ratio $\nu = 0.3$ and averaged mass density of the RPF layer 100 kg/m^3. The stress-strain curve used at the FEA is shown in Fig. 8. The shear modulus of the RPF depends on the elastic modulus (E) and Poisson's ratio (ν).

The mechanical properties of the ALF layer are Poisson's ratio $\nu = 0.3$ and averaged mass density of the ALF layer = 320 kg/m^3. The stress-strain curve used for the ALF is shown in Fig. 9.

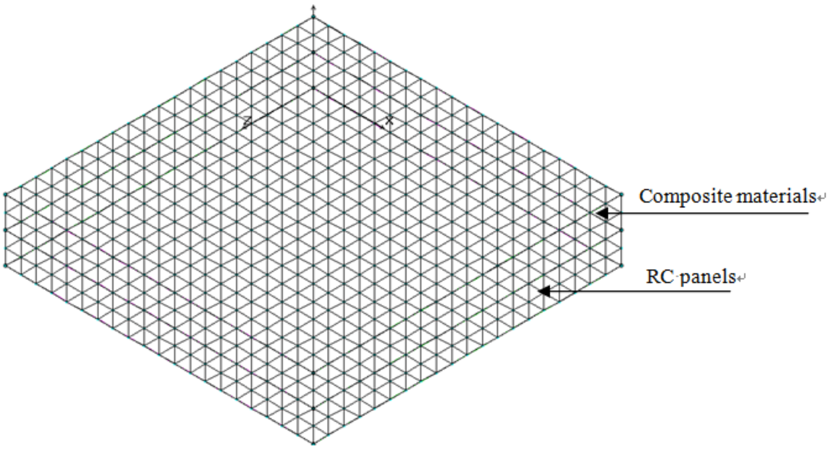

Fig. 7 3-D finite element model of the RC panels strengthened by composite materials

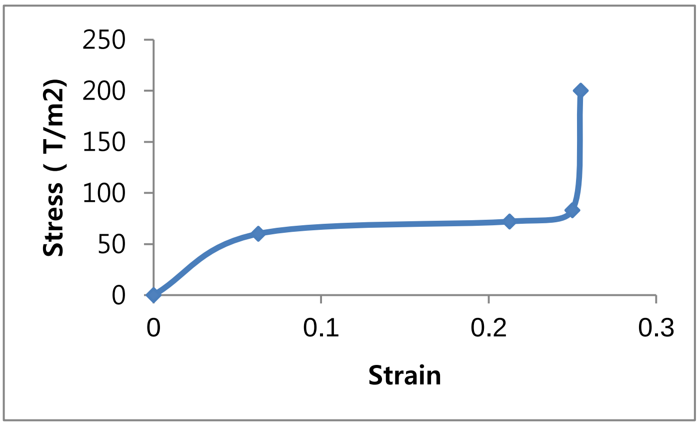

Fig. 8 Stress-strain curve of the rigid polyurethane foam (RPF)

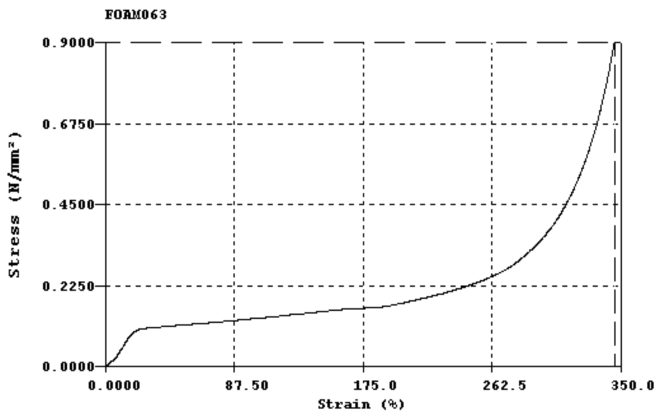

Fig. 9 Stress-strain curve of the aluminium foam (ALF)

The shear modulus of the ALF depends on the elastic modulus (E) and Poisson's ratio (ν).

The 3-D numerical model is chosen to reflect the behavior of the RC panel used in the field blast test. 1-kg TNT, 2-kg TNT, and 3-kg TNT explosives are used in the field blast test. The 3-D finite element mesh models the composite materials (the RPF and the ALF) and the RC panel length, width, and depth in x, y, and z directions, respectively, as shown in Fig. 7. The length and the width of the RC panel are 1 m, as shown in Fig. 7. The length and the width of the composite material are 1 m, as shown in Fig. 7.

4. Numerical model analysis

The shock of the blast wave is generated when the surrounding atmosphere is subjected to an extreme compressive pulse radiating outward from the centre of the explosion. The pressure–time history of a blast wave can be illustrated with a general shape, as shown in Fig. 10 (Gaissmaire 2003). The illustration is an idealization for an explosion in free air, as shown in Fig. 10. Transient pressure being greater than ambient pressure is defined as the overpressure (P_s) (Smith and Hetherington 1994). The peak overpressure (P_s) is the maximum value of the overpressure at a given location. The rise time to peak overpressure is less than microsecond (Baker *et al*. 1983).

In this study, the CONWEP numerical program (Technical Manual TM 5-885-1 1986) is used to calculate the pressure-time history effect on the RC panel based on different TNT explosive charges. The CONWEP is a collection of conventional weapons effect calculations from the equations and the curves of TM 5-885-1 (1986).

The study presents a comparison between the pressure-time histories obtained by the empirical method (EM) developed by Henrych (Beshara 1994), by the field blast test, and by the numerical model- CONWEP. The empirical method uses the scaled distance (Z) to calculate the peak overpressure, as written in Eq. 1 (Beshara 1994).

$$Z = \frac{R}{\sqrt[3]{W}} \tag{1}$$

Where; R is the stand-off distance from the centre of the explosion to a given location in meter and W is the weight of the explosive in kg.

The equations developed by Henrych (Beshara 1994) divide the analysis into three fields based on one-meter scaled distances (Z) as presented in Eqs. 2 to 4.

$$P_s = \frac{14.072}{Z} + \frac{5.540}{Z^2} - \frac{0.357}{Z^3} + \frac{0.00625}{Z^4}\ (bar) \qquad \text{(for 0.05< Z<0.3)} \tag{2}$$

$$P_s = \frac{6.194}{Z} - \frac{0.326}{Z^2} + \frac{2.132}{Z^3}\ (bar) \qquad \text{(for 0.3< Z< 1)} \tag{3}$$

$$P_s = \frac{0.662}{Z} + \frac{4.05}{Z^2} + \frac{3.288}{Z^3}\ (bar) \qquad \text{(for 1< Z< 10)} \tag{3}$$

The scaled distance (Z) is also used to determine the positive duration time (T_s) and the positive impulse (i_s) by using Fig. 11 (Smith and Hetherington 1994).

The comparison between the results obtained by the field blast test, the empirical method, and the numerical model is conducted to assess the accuracy of the numerical model. One-kg TNT, two-kg TNT, and three-kg TNT explosive charges are applied at stand-off distance of one meter to

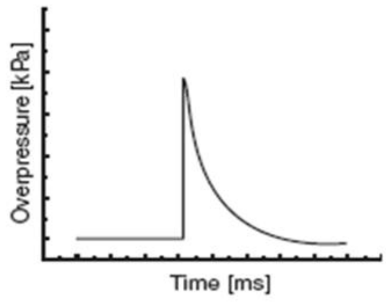

Fig. 10 Typical pressure time history in open air (after Gaissmaire 2003)

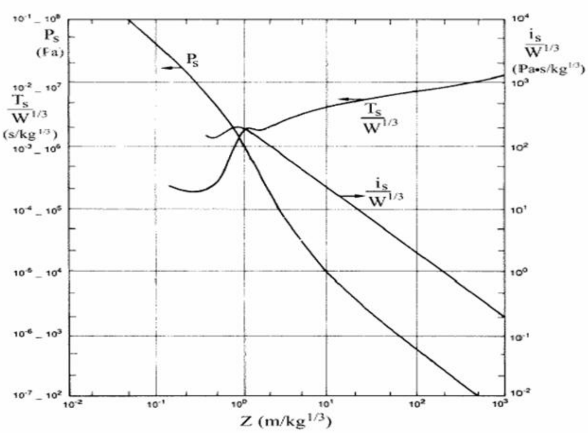

Fig. 11 Blast wave parameters for spherical charges of TNT (after Smith and Hetherington 1994)

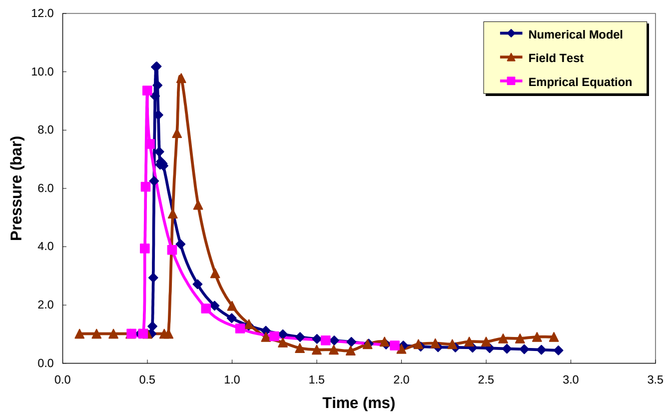

Fig. 12 Pressure-time history hitting the centre of the RC panel using 1-kg TNT explosive

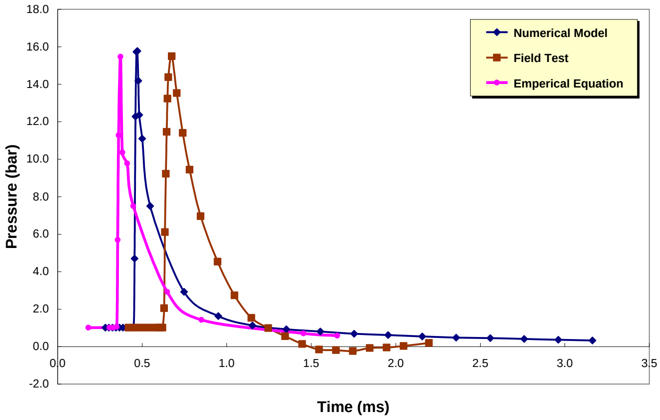

Fig. 13 Pressure-time history hitting the centre of the RC panel using 2-kg TNT explosive

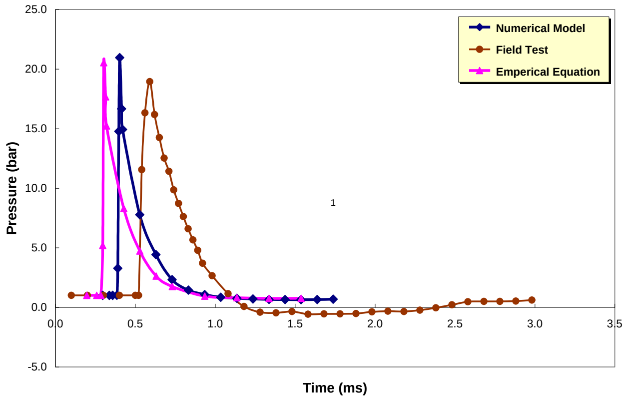

Fig. 14 Pressure-time history hitting the centre of the RC panel using 3-kg TNT explosive

obtain the pressure-time history hitting the RC panel by the EM, the numerical model, and the field blast test at the centre of the RC panel, as shown in Figs. 12 to 14. From these figures, it can be seen that the results obtained by the field blast test agree well with those estimated by both the numerical model and the EM.

5. Blast impact on performance of RC panel strengthened by composite materials

The maximum displacement at the centre of the control RC panel due to blast load is calculated using the 3-D FEA. The blast loads effect on the RC panel is shown in Figs. 12 to 14. The 3-D FEA is also used to calculate the maximum displacement at the centre of the RC panel strengthened by the composite materials (the RPF and the ALF) as structural retrofitting. The study discusses the impact of the RPF layer and the ALF layer on the RC panel performance under the blast impact. Three cases of the RC panel with and without the RPF layer and the ALF layer are studied. For the first case, the RC panel (control RC panel) is modelled without using the composite materials. For the second case, the RC panel is modelled using the RPF layer. For the third case, the RC panel is modeled using the ALF layer.

One-kg TNT explosive is used to discuss the impact of the RPF layer and the ALF layer on the RC panel (Figs. 1 and 2). The TNT explosive is located at the one-meter stand-off distance from the RC panel, as shown in Fig. 3. The pressure- time history hitting the RC panel is presented in Fig. 12. The maximum displacements at the centre of the RC panels for the three cases (Figs. 1 and 2) are computed to discuss the impact of the RPF layer and the ALF layer. Fig. 15 presents the comparison between the maximum computed displacements at the centre of the RC panels for each case. The maximum recorded displacement at the centre of the RC panel is also obtained by the field blast test, as shown in Fig. 16. The comparison indicates that the response of the RC panel strengthened by the RPF layer is lower than the response of the RC panel without the RPF layer, as shown in Figs. 15 and 16. The comparison indicates that the response of the RC panel strengthened by the ALF layer is lower than the response of the RC panel without the ALF layer, as shown in Figs. 15 and 16.

Two-kg TNT explosive is also used to discuss the impact of the RPF layer and the ALF on the RC panel (Figs. 1 and 2). Two-kg TNT explosive is also located at the one-meter stand-off distance from the RC panel, as shown in Fig. 3. The pressure-time history hitting the sandwich panel is also presented in Fig. 13. The maximum displacements at the centre of the RC panel based on the three cases (Figs. 1 and 2) are also calculated to discuss the impact of the RPF layer and the ALF. Fig. 15 shows the maximum computed displacements at the centre of the RC panels for each case. The maximum recorded displacement at the centre of the RC panel is obtained by the field blast test, as

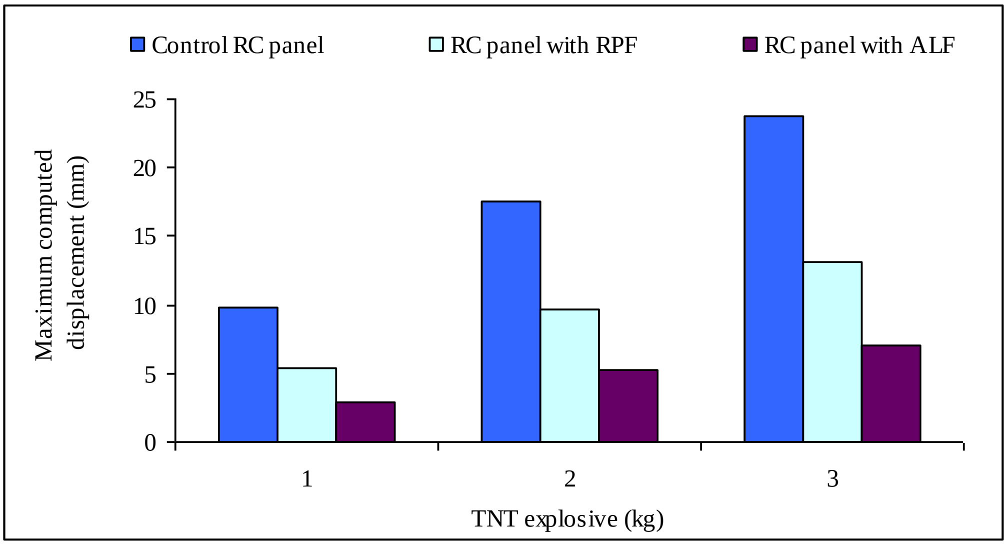

Fig. 15 Maximum computed displacement at the centre of RC panel strengthened by the RPF and the ALF layer under different TNT explosives

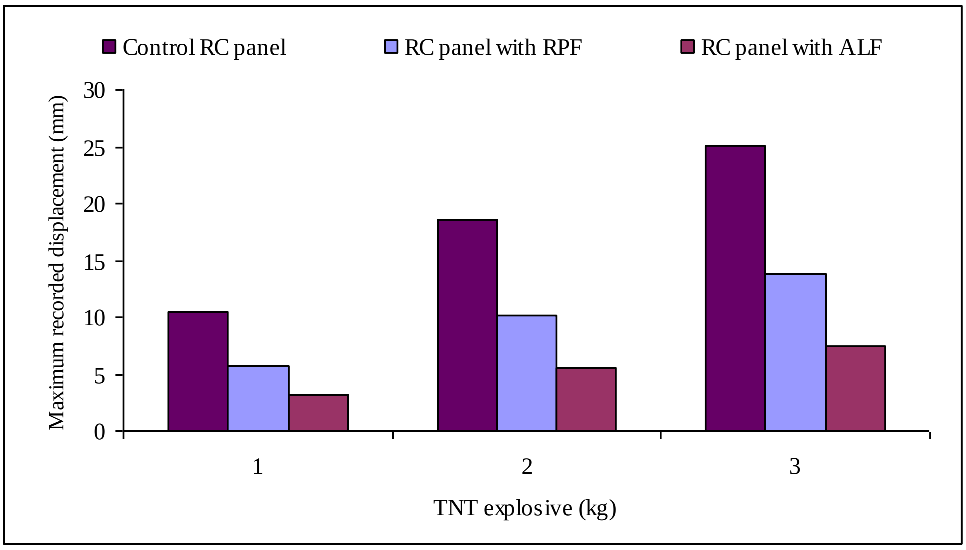

Fig. 16 Maximum recorded displacement at the centre of RC panel strengthened by the RPF and the ALF layer under different TNT explosives

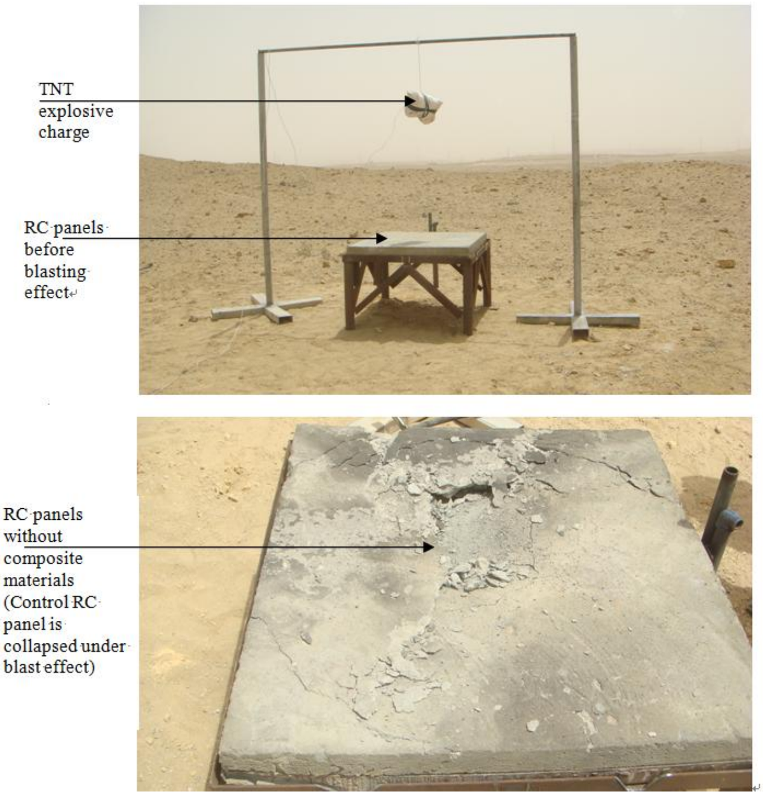

Fig. 17 Control RC panel subjected to 3-kg TNT explosive charge

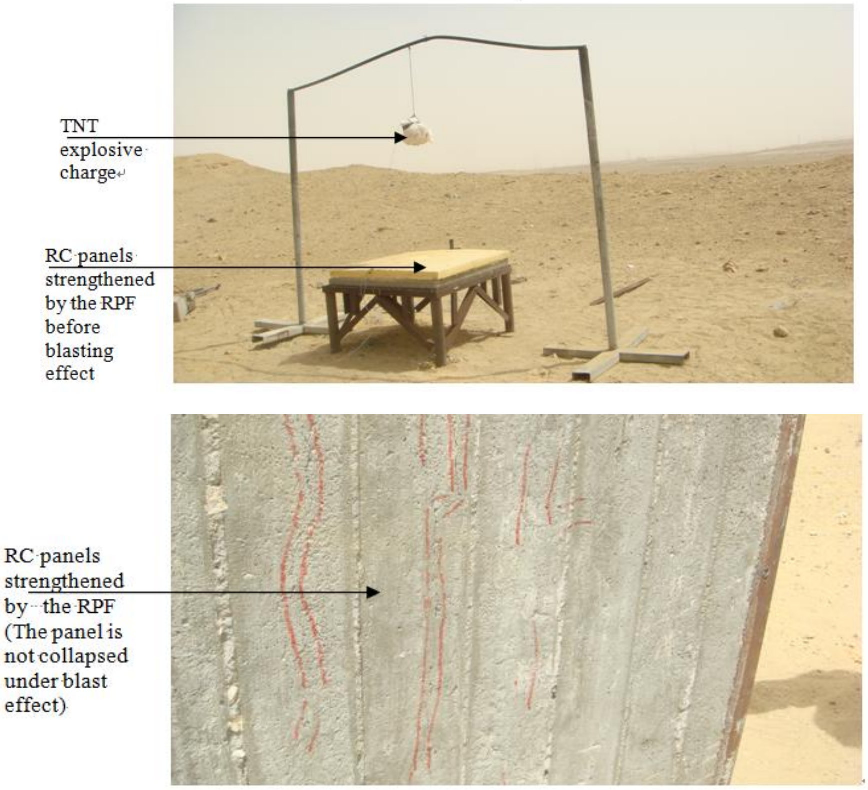

Fig. 18 RC panel strengthened by the RPF layer subjected to 3-kg TNT explosive charge

shown in Fig. 16. The comparison also shows that the response of the RC panel strengthened by the RPF layer is lower than the response of the RC panel without the RPF layer, as shown in Figs. 15 and 16. The comparison also shows that the response of the RC panel strengthened by the ALF layer is lower than the response of the RC panel without the ALF layer, as shown in Figs. 15 and 16.

Three-kg TNT explosive is again used to discuss the impact of the RPF layer and the ALF on the RC panels (Figs. 1 and 2). Fig. 17 shows the control RC panel subjected to 3-kg TNT explosive in the field blast test. The control RC panel is completely failed. Fig. 18 shows the RC panel strengthened by the RPF subjected to 3-kg TNT explosive. The RPF layer protects the RC panel from failure. The RPF layer absorbs the blast wave hitting the RC panel. Fig. 19 shows the RC panel strengthened by the ALF subjected to 3-kg TNT explosive. The ALF layer also protects the RC panel from failure. The ALF layer absorbs the blast wave hitting the RC panel. The comparison indicates that the response of the RC panel strengthened by the RPF layer is lower than the response of the RC panel without the RPF layer, as shown in Figs. 15 and 16. The comparison demonstrates that the response of the RC panel strengthened by the ALF layer is lower than the response of the RC panel without the ALF layer, as shown in Figs. 15 and 16. The results and the analysis also reveal that the performance of the RC panel strengthened by the ALF is better than this strengthened by the RPF, as shown in Figs. 15 and 16.

Fig. 19 RC panel strengthened by the ALF layer subjected to 3-kg TNT explosive charg

6. Discussions

The difference between the performance of the RC panels with and without the RPF layer and the ALF layer lies in the use of the RPF and the ALF. The RC panel (Figs. 1 and 2) is used to discuss the impact of the RPF layer and the ALF on the performance of the RC panel. The field blast test is conducted to study the performance of the RC panel strengthened by the RPF layer and the ALF and to trace the pressure-time histories hitting the RC panel based on different TNT explosive charges. The pressure-time history hitting the RC panel and the maximum displacement of the RC panel are recorded. The trends of the pressure-time histories obtained by the field blast test, the numerical model, and the empirical method are the same trend as those presented by Gaissmaire (2003).

Based on the field blast test, there is a good agreement between the recorded and the computed maximum displacement of the RC panel. The FEA gives a better estimation of the response of the RC panel strengthened by the RPF and the ALF.

In general, the RC panels play an important role to resist the blast load. The RPF layer improves the performance of the RC panel. The ALF layer also improves the performance of the RC panel. Therefore, the RPF layer and the ALF layer increase the RC panel stiffness and then reduce the displacement of the RC panel compared to the RC panel without the RPF layer and the

ALF layer. The RPF and the ALF have a large amount of strain energy which can absorb the kinetic energy of the blast wave propagation. Based on the field blast test and the 3-D FEA, the RPF reduces the maximum displacement of the RC panel by up to 45%. The ALF also reduces the maximum displacement of the RC panel by up to 70%.

The maximum displacement of the RC panel strengthened by the ALF is also smaller than this strengthened by the RPF. The strain energy of the ALF is higher than the strain energy of the RPF to absorb the blast wave energy. The response of the RC panel strengthened by the ALF layer is smaller than the response of the RC panel strengthened by the RPF layer by up to 40%. Finally, the performance of the RC panel is highly dependent on the material properties of both the RPF and the ALF which are used as a structural retrofitting.

7. Conclusions

A 3-D nonlinear finite element analysis has been used to predict the performance of RC panels with and without the PRF and the ALF layers under the blast effect. In this study, the performance of the RC panels strengthened by the composite material is modelled and analyzed using nonlinear finite element analysis. The following conclusions can be drawn regarding the performance of the RC panel strengthened by the composite material under impact of shock wave propagation in free air.

● The field blast test is conducted to study the performance of the RC panels strengthened by the composite material under different TNT explosive charges.

● The 3-D nonlinear FEA can be successfully used to analyze and estimate the performance of the RC panel based on the field blast test.

● Based on the field blast test and the empirical method developed by Henrych (Beshara 1994), the CONWEP numerical program gives a better estimate of the pressure-time history hitting the RC panel.

● The pressure-time histories calculated by the CONWEP numerical program (Technical Manual TM 5-885-1 1986) has the same trend as that presented by Gaissmaire (2003).

● The pressure-time histories calculated by the CONWEP numerical program is in reasonable agreement with those obtained by both the field blast test the empirical method developed by Henrych (Beshara 1994).

● The response of the RC panel strengthened by the RPF layer is reduced by up to 45% with respect to that of the RC panel without the RPF layer.

● The response of the RC panel strengthened by the ALF layer is reduced by up to 70% with respect to that of the RC panel without the ALF layer.

● The response of the RC panel strengthened by the ALF layer is smaller than the response of the RC panel strengthened by the RPF layer by up to 40%.

However, the rigid polyurethane foam (RPF) and the aluminum foam (ALF) could be used as structural retrofitting to absorb the energy of the blast wave propagation hitting the reinforced concrete structures.

Acknowledgement

The authors acknowledge the Egyptian Engineering Department for its assistance in providing technical information. Part of the funding for this research is provided by Military Technical College and the Egyptian Engineering Department.

References

Aimone, C.T. (1982), “Three-dimensional wave propagation model of full-scale rock fragmentation”, Ph.D. Thesis, Northwestern University.

Baker, W.E., Cox, P.A., Kulesz, J.J. and Strehlow, R.A. (1983), “Explosion hazards and evaluation”, Elsevier.

Beshara, F.B.A. (1994), “Modeling of blast loading on aboveground structures -I. Internal blast and ground shock”, *Compos. Struct.*, **51**(5).

Chen, H. (Roger) and Chen S. (1996), “Dynamic responses of shallow-buried flexible plates subjected to impact loading”, *J. Struct. Eng.*, January 1996, 55-60.

Dharmasena, K.P., Wadley H.N., Xue, Z., John, W. Hutchinson, J.W. (2008), “Mechanical response of metallic honeycomb sandwich panel structures to high-intensity dynamic loading”, *Int. J. Impact Eng.*, **35**(2008) 1063-1074.

Fayad, H.M. (2009), *The Optimum Design of the Tunnels Armoured Doors under Blast Effects*, Ph. D. Thesis. Military Technical College (MTC). Cairo

Gaissmaiere, A.E.W. (2003), “Aspects of thermobaric weapon”, ADF Health, Vol. 4, pp. 3-6.

Gustafsson, R. (1973), Swedish Blasting Technique, Gothenburg, Sweden, SPI.

Ha, J., Yi N., Choi, J. and Kim, J. (2011), “Experimental study on hybrid CFRP-PU strengthening effect on RC panels under blast loading”, *J. Compos. Struct.*, **93**, 2070-2082.

Hao, H., Ma, G.W. and Zhou, Y.X. (1998), “Numerical simulation of underground explosions”, *Fragblast the Int. J. Blasting Fragment.*, **2**, 383-395.

Laine L. and Hedman O. (1999), *Finite Element Calculation of Swedish Rescue Centers (RC 90) and Shelters*, 3rd Asia-Pacific Conference on Shock & Impact Loads on Structures, 205-212, November24-26, Singapore.

Liu, L. and Katsabanis, P.D. (1997), “Development of a continuum damage model for blasting analysis”, *Int. J. Rock Mech. Min. Sci.*, **34**, 217-231.

Lu, Y., Wang, Z., and Chong, K. (2005), A comparative study of buried structure in soil subjected to blast load using 2-D and 3-D numerical simulations, *J. Soil Dyn. Earthq. Eng.*, **25**. 275-288.

Luccioni, B., Ambrosini, D., Nurick, G. and Snyman, I. (2009), “Craters produced by underground explosions”, *J. Comput. Struct.*, **87**, 1366-1373.

Mazek, S. and Mostafa, A. (2013), Impact of a shock wave on a structure strengthened by rigid polyurethane foam, *J. Struct. Eng. Mech.*, **48**(4)569-585.

Mazek, S.A. (2014), “Performance of sandwich structure strengthened by pyramid cover under blast effect”, *J. Struct. Eng. Mech.*, **50**(4), 471-486.

Ming, W.H. (2008), “Investigation on the blast resistance of a stiffened door structure”, *J. Marine Sci. Tech.*, **16**(2), 149-157.

Mohamad, L.S. (2006), Study and design of fortified structures due to blast effects. M.Sc thesis. Military Technical College (MTC). Cairo. Ammunition and Explosives. In document: AC/258-D/258, Brussels, Belgium.

Remennikov, A. (2003), “A review of methods for predicting bomb blast effects on buildings”, *J. battlefield Tech.*, **6**(3), 155- 161.

Schueller, C.T. (1991), Structural Dynamics. Springer-Verlag, Berlin, New York, ISBN 0-387-

53593-4.
Smith, P.D. and Hetherington, J.G. (1994), Blast and ballistic loading of structures. Butterworth-Heinemann Ltd. UK.
Technical Manual TM 5-885-1. 1986. Fundamentals of Protective Design for Conventional Weapons. Headquarters Department of the Army, Washington DC.
Technical Manual TM 5-1300. 2008. Structures to Resist the Effects of Accidental Explosions. Unified Facilities Criteria (UFC) .U.S. Army Corps of Engineers; Naval Facilities Engineering Command; Air Force Civil Engineer Support Agency.
Trelat, S., Sochet, I., Autrusson, B., Cheval, K. and Loiseau, O. (2007), "Impact of a shock wave on a structure on explosion at altitude", *J. Loss Prevention on the Process Industries*, **20**, 509-516.
Wu, C., Hao, H. and Zhou, Y.X. (1999), "Dynamic response analysis of rock mass with stochastic properties subjected to explosive loads", *Fragblast the Int. J. Blasting Fragment.*, **3**, 137-153.
Zhang, W. and Valliappan, S. (1990), "Analysis of random anisotropic damage mechanics problems of rock mass, Part II: Statistical estimation", *Rock Mech. Rock Eng.*, **23**, 241-259.

CC